

## Heterogeneous nucleation as a potential sulphate-coating mechanism of atmospheric mineral dust particles and implications of coated dust on new particle formation

H. Korhonen,<sup>1</sup> I. Napari,<sup>1</sup> C. Timmreck,<sup>2</sup> H. Vehkamäki,<sup>1</sup> L. Pirjola,<sup>1,3</sup>  
K. E. J. Lehtinen,<sup>1</sup> A. Lauri,<sup>1</sup> and M. Kulmala<sup>1</sup>

Received 3 March 2003; revised 26 May 2003; accepted 4 June 2003; published 10 September 2003.

[1] The plausibility of heterogeneous nucleation of water, sulphuric acid, and ammonia as a pathway leading to soluble coating of atmospheric mineral dust is investigated. In addition, the effect of such sulphate-coated dust on the formation and growth of atmospheric aerosol particles is addressed. The simulated new particle formation mechanism is ternary nucleation of water, sulphuric acid, and ammonia vapors, while in the condensational growth process the effect of condensable organic vapor is also studied. The results indicate that soluble coating of dust by heterogeneous nucleation can occur at atmospheric sulphuric acid concentrations. In addition, the simulations show that homogeneous ternary nucleation and subsequent growth are decoupled. Although observed (or even higher) dust concentrations are unable to inhibit new particle formation, coated dust particles acting as condensation and coagulation sinks can prevent the growth of newly formed particles to detectable sizes. This is particularly true in desert areas, where organic vapor concentrations are low.

*INDEX TERMS:* 0305 Atmospheric Composition and Structure: Aerosols and particles (0345, 4801); 0365 Atmospheric Composition and Structure: Troposphere—composition and chemistry; 3210 Mathematical Geophysics: Modeling; *KEYWORDS:* aerosol, mineral dust, soluble coating, heterogeneous nucleation, particle formation and growth, condensation sink

**Citation:** Korhonen, H., I. Napari, C. Timmreck, H. Vehkamäki, L. Pirjola, K. E. J. Lehtinen, A. Lauri, and M. Kulmala, Heterogeneous nucleation as a potential sulphate-coating mechanism of atmospheric mineral dust particles and implications of coated dust on new particle formation, *J. Geophys. Res.*, 108(D17), 4546, doi:10.1029/2003JD003553, 2003.

### 1. Introduction

[2] Mineral aerosols play an important role in the global climate system, and changes in their atmospheric concentration are largely due to anthropogenic impact, such as wind erosion of agricultural land, deforestation, salinization, overgrazing, and urbanization [Andreae, 1996; Tegen *et al.*, 1996]. Of the total global dust emissions estimated to range from 1000 Mt/yr to 5000 Mt/yr [Duce, 1995] with high variability in time and space, human activities account for 30 to 50 percent [Tegen and Fung, 1995]. This estimate of the anthropogenic contribution is, however, highly uncertain [Intergovernmental Panel on Climate Change (IPCC), 2001].

[3] Dust aerosols disturb the radiative balance of the atmosphere by absorbing and scattering incoming solar radiation and by absorbing and emitting outgoing thermal

radiation. It is, however, still impossible to quantify the radiative forcing of the dust particles [Sokolik *et al.*, 2001]. Magnitude and sign of the forcing depend on the optical properties (as a function of particle size distribution and refractive index) and on the albedo of the underlying surfaces including cloud cover [Tegen and Lacis, 1996; Sokolik and Toon, 1996; Liao and Seinfeld, 1998; Claquin *et al.*, 1998]. In addition, the mineral dust particles can in multiple ways have an indirect effect on the climate system. Model studies show that mineral aerosol could significantly affect atmospheric chemistry, in particular that of ozone and nitrogen compounds [Dentener *et al.*, 1996; Zhang and Carmichael, 1999; Underwood *et al.*, 2001]. Dust has also a potentially strong impact on the major biogeochemical cycles because the deposition of micronutrients (e.g., Fe, Si, P) can change the productivity of marine [e.g., Martin, 1991; Coale *et al.*, 1996] and terrestrial [e.g., Chadwick *et al.*, 1999] ecosystems.

[4] Measurements in the eastern Mediterranean have revealed that mineral dust particles get often coated with sulphate and other soluble material [Levin *et al.*, 1996]. Soluble coating enables the dust particles to serve as cloud condensation nuclei (CCN) and could therefore change their impact on the microphysical development of other

<sup>1</sup>Department of Physical Sciences, University of Helsinki, Helsinki, Finland.

<sup>2</sup>Max-Planck-Institut für Meteorologie, Hamburg, Germany.

<sup>3</sup>Department of Technology, Helsinki Polytechnic Stadia, Helsinki, Finland.

clouds and the formation of rainfall [Wurzler *et al.*, 2000]. While the mechanism responsible for the soluble coating is still uncertain, observations have shown that the amount of soluble material on dust particles correlates with particle surface area [Levin *et al.*, 1996]. Simulations of Wurzler *et al.* [2000] indicated that impaction scavenging by cloud droplets initially formed on soluble particles is a possible pathway for the soluble coating of the mineral dust particles. Other suggested coating mechanisms, which are consistent with the occasional observations of a patchy rather than uniform sulphate coating [Levin *et al.*, 1996], include coagulation of dust and sulphate particles, and oxidation of SO<sub>2</sub> to SO<sub>4</sub> on dry mineral aerosol [Dentener *et al.*, 1996].

[5] The explanation to patchy coating may also lie in heterogeneous nucleation of vapor mixtures containing sulphate, a process in which liquid embryos form on insoluble surfaces. This coating pathway has long been neglected, mainly because of the formation energy barrier associated with its onset. Recent theoretical calculations [Coffman and Hegg, 1995; Napari *et al.*, 2002] and preliminary experimental findings [Ball *et al.*, 1999] indicate, however, that conucleation of sulphuric acid, ammonia, and water is capable of producing new particles at atmospheric conditions. As heterogeneous nucleation on surfaces can take place at significantly lower supersaturations, its plausibility as a dust-coating mechanism is worthy of consideration. The onset of this mechanism is strongly dependent on the characteristics of the mineral dust surface, varying in shape and consistency. Heterogeneous nucleation therefore provides a consistent picture with the observation that only a few of the mineral particles have soluble coating on them [Levin *et al.*, 1996].

[6] The research focused on soluble coated dust particles has not thus far addressed their impact on aerosol microphysics and on new particle formation in particular. Analyses of nucleation events have, however, emphasized the importance of pre-existing particles acting as condensation and coagulation sinks during new particle formation [Kulmala *et al.*, 2001a, 2001b], and therefore the relatively large soluble coated dust particles may notably influence the growth and detection of newly formed particles. This could be particularly evident if the dust layer is enhanced after strong dust events. Measurements [D'Almeida and Schütz, 1983] show for dust storm events an increase in the particle number density by more than an order of magnitude.

[7] In this paper, we investigate the plausibility of heterogeneous conucleation of H<sub>2</sub>SO<sub>4</sub>, NH<sub>3</sub>, and H<sub>2</sub>O as a possible pathway leading to sulphate coating of mineral aerosol particles. Furthermore, we apply a detailed aerosol dynamics model to look into the effect of soluble coated mineral dust particles on aerosol microphysics and in particular on new particle formation and growth. We aim to find theoretical estimates for dust concentrations sufficient to inhibit new particle formation by homogeneous ternary nucleation or to prevent the growth of formed particles to detectable sizes. The following section briefly summarizes the theory of heterogeneous nucleation and discusses its potential for coating dust particles with soluble material. Section 3 describes the aerosol dynamics

model and section 4 presents the model results. Section 5 summarizes the major outcomes of this study.

## 2. Heterogeneous Nucleation

[8] Recent studies have shown that apart from very low temperatures, e.g., in the free troposphere, ternary nucleation of sulphuric acid-ammonia-water mixture can take place at significantly lower supersaturations than binary nucleation of sulphuric acid and water [Ball *et al.*, 1999; Napari *et al.*, 2002]. In this study, we therefore consider soluble coating of mineral dust particles by heterogeneous vapor-liquid nucleation of H<sub>2</sub>SO<sub>4</sub>, NH<sub>3</sub>, and H<sub>2</sub>O. The nucleation scheme applied builds on a recently revised model for ternary homogeneous nucleation [Napari *et al.*, 2002]. The critical radii of the forming embryos are the same for heterogeneous and homogeneous nucleation mechanisms. To determine the free energy involved in the formation of a heterogeneous embryo, however, one must account for the different surface to volume ratio and the influence of the liquid-solid interface. The nucleation model of Napari *et al.* [2002] is based on a thermodynamically consistent version of the classical nucleation theory. Although the classical theory has its well-known shortcomings, some of which new theoretical approaches [Laaksonen and Oxtoby, 1995] are capable of addressing, it is still the only one applicable to atmospheric models.

### 2.1. Theory

[9] We follow the theoretical formulations of heterogeneous nucleation by Fletcher [1958], Hamill *et al.* [1982], and Kulmala *et al.* [2001c], who assume that nucleation proceeds via direct vapor deposition onto the particle surface. For practical reasons, the nucleating embryo is treated as a portion of a sphere, and the substrate particle as a sphere with energetically homogeneous surface. The latter assumption introduces some error in the formulation because, in reality, the heterogeneous nucleation rate depends strongly on the characteristics of the underlying surface. However, because the interactions between the nucleating molecules and the energetically heterogeneous surface are complex and difficult to quantify, assuming homogeneity throughout the substrate surface is customary in atmospheric models. Despite this deficiency, the formulation should allow attainment of qualitatively reliable results on the formation of liquid embryos on solid particle surfaces.

[10] To determine the critical size of the forming embryo on a spherical substrate particle of radius  $R_p$ , consider an embryo consisting of  $n = \sum_i n_i$  molecules, where  $n_i$  stands for the number of molecules of the nucleating compound  $i$ . Minimizing the formation free energy of the embryo with respect to all variables  $n_i$  gives [Fletcher, 1958]

$$\Delta G^* = \frac{2\pi}{3} r^* \sigma_{12} f(m, z), \quad (1)$$

where  $\Delta G^*$  is the formation energy and  $r^*$  the radius of the critical embryo, and  $\sigma_{12}$  the surface tension between the embryo phase and the surrounding gas phase. Equation (1)

takes the geometry of the forming embryo into account through the factor

$$f(m, z) = 1 + \left(\frac{1 - mz}{g}\right)^3 + z^3 \left[ 2 - 3\left(\frac{z - m}{g}\right) + \left(\frac{z - m}{g}\right)^3 \right] + 3mz^2 \left(\frac{z - m}{g} - 1\right), \quad (2)$$

where

$$g = (1 + z^2 - 2mz)^{1/2}, \quad (3)$$

$$z = \frac{R_p}{r^*} \quad (4)$$

and

$$m = \cos \theta = \frac{\sigma_{13} - \sigma_{23}}{\sigma_{12}}. \quad (5)$$

In equation (5),  $\theta$  is the contact angle, which is determined by the interfacial free energies  $\sigma_{ij}$ . Index 1 stands for the gas phase, index 2 for the embryo phase, and index 3 for the substrate phase. In the lack of measured values for the interfacial free energies in the case of ternary heterogeneous nucleation on mineral dust, it is of great importance to assess the sensitivity of the model results to the contact angle value chosen in the model. On completely wettable surfaces, corresponding to contact angle  $0^\circ$ , heterogeneous nucleation is an effective coating mechanism whereas nucleation on completely unwettable surface with a contact angle  $180^\circ$  corresponds to homogeneous nucleation.

[11] In the formulation of *Hamill et al.* [1982], the triggering mechanism for liquid embryo formation is adsorption of vapor molecules onto the solid particle surface, and the number of molecules adsorbed per unit area is given by

$$N_{ads} = \sum_i \beta_i \tau_i = \sum_i \frac{\beta_i}{\nu_i} \exp(E_i/RT). \quad (6)$$

In this equation,  $\beta_i$  is the impinging rate and  $\tau_i$  the residence time of the molecules of compound  $i$  on the substrate particle surface. At a given temperature  $T$ , the residence time can be expressed with the help of the heat of adsorption,  $E_i$ , and the characteristic frequency of vibration of the molecules,  $\nu_i$  [*Lazaridis et al.*, 1991]. This frequency between two molecules can be calculated using the nearest-neighbor harmonic oscillator approximation. For  $E_i$ , we used the latent heat of condensation given by *Adamson* [1982]. Correspondingly, at 275 K the calculated values for  $\nu_i$  and  $E_i$  were  $3.92 \times 10^{12} \text{ s}^{-1}$  and 44 970 J/mol for water,  $1.16 \times 10^{12} \text{ s}^{-1}$  and 84 340 J/mol for sulphuric acid, and  $3.92 \times 10^{12} \text{ s}^{-1}$  and 21750 J/mol for ammonia, respectively. Although the determination of the number of vapor molecules adsorbed suffers from uncertainty related to the nature of the substrate particle, *Hamill et al.* [1982] evaluated the uncertainty in the contact angle value much more significant.

[12] This study assumed that heterogeneous nucleation takes place once critically sized soluble nuclei cover the entire dust particle surface. The heterogeneous nucleation rate consistent with this assumption is

$$I = \pi r^* 2 N_{ads} R_{av} Z N_p \exp\left(-\frac{\Delta G^*}{kT}\right), \quad (7)$$

corresponding to the maximum time for nucleation. The rate that corresponds to the minimum time for nucleation defines the rate at which a single critical embryo forms on a solid particle surface. Then, the heterogeneous nucleation rate is

$$I = 4\pi R_p^2 N_{ads} R_{av} Z N_p \exp\left(-\frac{\Delta G^*}{kT}\right). \quad (8)$$

For our purposes this formulation is not, however, well-suited since one critically sized embryo covers only a small fraction of the dust particle surface area and cannot therefore be considered to coat the whole dust surface with soluble material. In the equations above,  $R_{av}$  denotes the average condensation rate on the embryo,  $Z$  the Zeldovich nonequilibrium factor [*Arstila et al.*, 1999], and  $N_p$  the number concentration of substrate particles. For the purpose of this study, an important concept is the probability that heterogeneous nucleation occurs within time  $\Delta t$ . This nucleation probability

$$P = 1 - \exp(-I\Delta t) \quad (9)$$

allows us to determine the portion of the dust particle population that has been coated with soluble material at a certain time.

## 2.2. Soluble Coating of Mineral Dust Particles

[13] To evaluate the potential of heterogeneous nucleation to coat atmospheric mineral dust particles with soluble material, we applied equations (7) and (9) to study the conucleation of sulphuric acid, ammonia, and water. In determining the onset of heterogeneous nucleation, of key importance is the interaction between the forming embryo and the dust particle. Figure 1 demonstrates that depending on the strength of this interaction, taken into account through the contact angle  $\theta$  in the nucleation model, the concentrations of sulphuric acid and ammonia required for soluble coating vary markedly. Even then, all the calculated critical sulphuric acid concentrations shown in the figure, irrespective of the contact angle value, are within or below the typically measured range of  $10^5 - 10^7 \text{ cm}^{-3}$  [*Eisele and Tanner*, 1993; *Weber et al.*, 1997]. An increase in ammonia mixing ratio from 1 ppt (Figure 1a) to 5 ppt (Figure 1b) lowers the sulphuric acid concentration required for soluble coating by an order of magnitude for each respective contact angle value. The temperature chosen for the calculations, 275 K, corresponds crudely to that at altitudes where *Levin et al.* [1996] detected soluble coated dust. One should note, however, that the nucleation probability curves are temperature dependent and shift to right when temperature rises. In contrast, the substrate particle size has very little influence on the results in the dust size range.



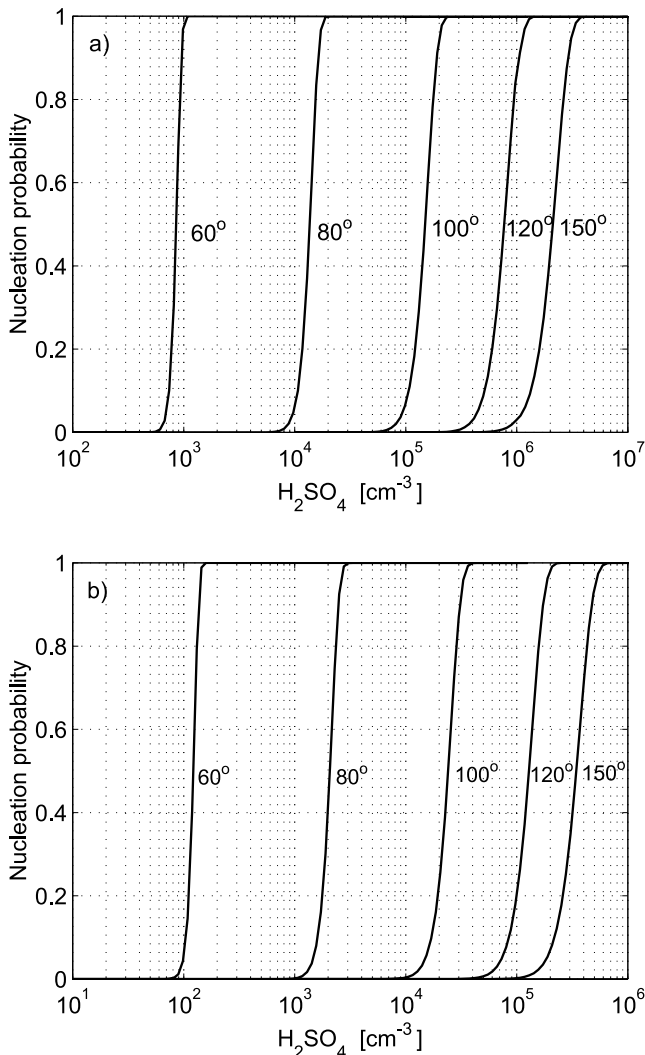


**Figure 1.** Probability of heterogeneous nucleation as a function of contact angle and sulphuric acid concentration at temperature 275 K, relative humidity 50%, and ammonia mixing ratios (a) 1 ppt and (b) 5 ppt. In the calculations, the substrate particle diameter was 1  $\mu\text{m}$ , and the time period in consideration was 1 s.

[14] Although the simulation results predict soluble coating of dust particles at very low sulphuric acid concentration, dust without soluble coating is frequently observed in the atmosphere. Our formulation of heterogeneous nucleation based on the self-consistent classical nucleation theory therefore seems to somewhat overestimate its coating potential. While this may to some extent arise from the insufficient data available to describe the interaction between the nucleating molecules and the substrate surface, another factor to keep in mind is that at low vapor concentrations, condensation onto the forming embryos is very slow and condensational growth and nucleation are decoupled [Kulmala *et al.*, 2000]. Under such conditions, the formation of observable soluble coating requires additional condensable species or very long timescales. For sulphuric acid condensation at concentrations above  $10^5 \text{ cm}^{-3}$ , however, these obstacles vanish, and on the basis of our simulations, ternary

heterogeneous nucleation seems a possible pathway of sulphate coating.

### 3. Aerosol Dynamics Model

[15] The impact of soluble coated mineral dust on aerosol dynamics, and on new particle formation events in particular, was investigated with a zero-dimensional aerosol dynamics and gas-phase chemistry model MONO32 [Pirjola and Kulmala, 2000; Pirjola *et al.*, 2003]. In this model, particles can contain both soluble and insoluble material; same sized particles are, however, uniform in composition. Aerosol dynamics processes included are homogeneous ternary  $\text{H}_2\text{SO}_4\text{-H}_2\text{O-NH}_3$  nucleation, heterogeneous ternary nucleation on mineral dust particles, multicomponent condensation, coagulation, and dry deposition. The calculation of homogeneous and heterogeneous nucleation rates builds on the recently revised ternary nucleation model of Napari *et al.* [2002]. Of the condensable compounds, sulphuric acid has a negligible vapor pressure while the organic vapor can be either nonvolatile, semivolatile, or highly volatile. The current version of the model neglects the condensation of ammonia. An empirical fit [Tang and Munkelwitz, 1994] for the solute mass fraction as a function of water activity determines the water content of the particles. Calculation of Brownian coagulation coefficients follows the formulation of Fuchs [1964]. The scheme for dry deposition of particles takes into account Brownian diffusion, interception, and gravitational settling [Schack *et al.*, 1985].

[16] MONO32 has been developed to simulate aerosol processes in 1-D boundary layer and 3-D Eulerian models. To minimize computational costs in such large codes, it represents each particle mode (nucleation, Aitken, accumulation, coarse) with a single moving monodisperse size section. As is well-known, the moving size bin method is an excellent choice for simulation of condensational growth of particles. Continuous nucleation, however, causes problems if the first formed particles grow because of condensation and self-coagulation and leave no size bin small enough to put freshly nucleated particles into. Placing these particles into the nucleation mode with the pre-existing ones requires conservation of number and mass, and thus the monodisperse method somewhat underestimates the growth of earlier nucleated particles. In simulations focusing on nucleation mode particle growth to a certain detectable size, it is therefore necessary to concentrate on short nucleation bursts only. Another option, creating a new size bin for the freshly nucleated particles after each time step, raises the computational cost of the approach considerably.

## 4. Impact of Dust On Aerosol Dynamics

### 4.1. Simulation Conditions

[17] To investigate new particle formation and growth in the presence of relatively large mineral dust particles, we simulated particle formation by homogeneous nucleation simultaneously with other aerosol dynamics. Heterogeneous nucleation, for which we chose a constant contact angle value  $100^\circ$ , was essential in the simulations because water-soluble material, such as sulphuric acid and organic compounds, could start condensing onto dust particles only after the particles had gained soluble coating.

[18] In each 6-hour simulation, run from 9 a.m. to 3 p.m., the temperature was 275 K and relative humidity 50%. Oxidation of sulphur dioxide ( $\text{SO}_2$ ) by hydrate radicals (OH) and subsequent reactions provided a source for sulphuric acid. The radical had a semisinusoidal diurnal pattern, which peaked at noon with a value of  $10^6 \text{ cm}^{-3}$ . Sulphur dioxide concentration, on the other hand, was constant in each individual simulation but varied between the simulations from  $5 \times 10^7$  to  $1.3 \times 10^{10} \text{ cm}^{-3}$  (1.9 to 490 ppt) [e.g., Wurzler et al., 2000; Alam et al., 2003]. In addition to sulphuric acid, a semivolatile organic compound, with molar mass 102.2 g/mol and equilibrium vapor concentration  $2 \times 10^5 \text{ cm}^{-3}$ , condensed onto the particles. Although the organic compounds contributing to particle growth have not been identified, modeling work has shown that in order to condense onto nanometer range particles the equilibrium vapor concentration has to be below  $10^5$ – $10^6 \text{ cm}^{-3}$  [Kerminen et al., 2000; Pirjola and Kulmala, 2001]. The modeled organic compound was partly water-soluble and its production rate had a semisinusoidal pattern. The noontime peak values for the organic production rates ranged from  $4.3 \times 10^3$  to  $1.0 \times 10^5 \text{ cm}^{-3} \text{ s}^{-1}$ , which is in accordance with field measurements [Kulmala et al., 2001a; O'Dowd et al., 2002]. The mixing ratio of ammonia was 5 ppt.

[19] Three monodisperse size modes approximated the pre-existing particle size distribution. In Aitken and accumulation modes, the initial number concentrations and diameters of sulphuric acid-water particles were  $800 \text{ cm}^{-3}$  and 29 nm, and  $200 \text{ cm}^{-3}$  and 146 nm, respectively. For the dust aerosol size distribution, only a few detailed studies exist thus far. Although very large dust particles up to 100 and 1000  $\mu\text{m}$  in diameter with relatively short residence times have been detected near the sources [Duce, 1995], several thousand kilometers downwind from these areas the typical mass mean diameter of the mineral aerosol is between 1 and 3  $\mu\text{m}$  [Schütz et al., 1981; Prospero et al., 1989]. Measurements of the submicron particle number size distribution [D'Almeida and Schütz, 1983; Gomes et al., 1990] show a peak around 0.1  $\mu\text{m}$  (0.05–0.15  $\mu\text{m}$ ) and particles as small as 0.02  $\mu\text{m}$  in diameter. In our simulations, the dust particle diameter ranged from 200 nm to 10  $\mu\text{m}$ .

[20] Although a typical atmospheric dust distribution expands over several orders of magnitude in size, in the monodisperse model a single particle size represents the contribution of all the dust particles to various aerosol processes dependent on either particle size, surface area, or volume. Therefore, rather than focusing on the dust number concentrations predicted by the model, we chose the condensation sink as a primary measure of the dust loading. The condensation sink, defined as the rate at which vapor molecules condense onto aerosol particles, has been shown to be a good measure of the scavenging of condensable vapor as well as freshly nucleated particles onto the existing background aerosol [Kulmala et al., 2001a]. It has an expression

$$CS = 4\pi D \sum_i \beta_i r_i N_i, \quad (10)$$

where  $D$  stands for the vapor diffusion coefficient,  $r_i$  and  $N_i$  for the radius and number concentration of particles of size

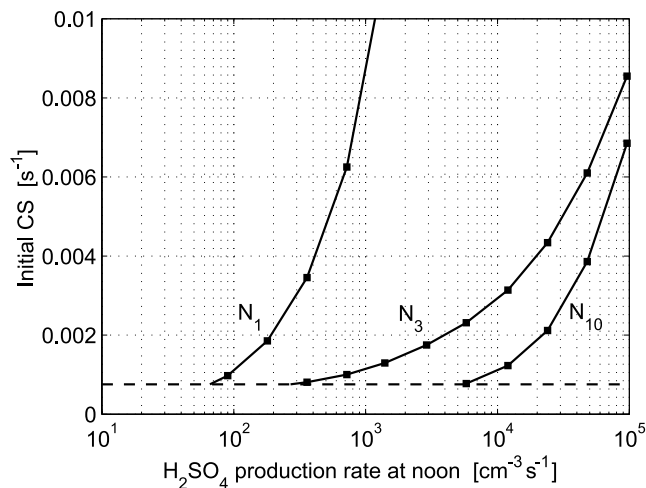


**Figure 2.** Critical initial condensation sinks that prevent the formation of new particles by homogeneous nucleation ( $N_1$ ), and growth of nucleated particles to 3 and 10 nm ( $N_3$  and  $N_{10}$ , respectively) as a function of sulphuric acid production rate. The results are shown for substrate particles of 1  $\mu\text{m}$  in diameter. See text for detailed simulation conditions.

$i$ , and  $\beta_i$  for the transitional correction factor according to Fuchs and Sutugin [1971]. Calculations using the typical clean and polluted environment particle size distributions [Seinfeld and Pandis, 1998] indicate that condensation sinks in the atmosphere typically range from  $10^{-4}$  to  $10^{-2} \text{ s}^{-1}$  although in highly polluted areas the sink value can rise even higher (P. Mönkkönen, manuscript in preparation, 2003).

## 4.2. Results and Discussion

[21] First, we aimed to find out at which conditions atmospheric mineral aerosols can provide such a high condensation sink for nucleating vapors that it prevents new particle formation by homogeneous nucleation altogether (homogeneous nucleation, i.e., formation of approximately 1 nm sized clusters, is denoted  $N_1$  hereafter). Second, we applied the aerosol dynamics model to predict the minimum condensation sinks and corresponding dust concentrations required to inhibit the growth of newly formed particles to detectable diameters of 3 and 10 nm ( $N_3$  and  $N_{10}$ , respectively) during the six-hour simulation. Finally, we tested the sensitivity of our base case results to some of the model parameters.

[22] In the base case simulations, the organic production rate had a noontime peak of  $8.7 \times 10^3 \text{ cm}^{-3}$ . Figure 2 summarizes the results in respect to minimum initial condensation sinks. Sinks sufficient to prevent the formation of  $N_1$ ,  $N_3$ , or  $N_{10}$  lie above the respective curves. Correspondingly, with sink values below the curves, the nucleation mode particles can form or grow to detectable sizes. The dashed line at the bottom of the figure corresponds to the condensation sink by Aitken and accumulation mode particles. The figure shows the model results for dust particles 1  $\mu\text{m}$  in diameter. Repetition of model runs for dust sizes 200 nm, 5  $\mu\text{m}$  and 10  $\mu\text{m}$  revealed, however, that although the critical initial sink

**Table 1.** Dust Concentrations Corresponding to Critical Initial Condensation Sinks in Figure 2 for Dust Particles of Diameter 200 nm, 1  $\mu\text{m}$ , and 5  $\mu\text{m}$ <sup>a</sup>

|                 | Maximum Sulphuric Acid Production Rate, $\text{cm}^{-3} \text{s}^{-1}$ |                   |                   |                   |                   |
|-----------------|--|-------------------|-------------------|-------------------|-------------------|
|                 | $9.0 \times 10^1$  | $3.6 \times 10^2$ | $1.4 \times 10^3$ | $5.8 \times 10^3$ | $2.4 \times 10^4$ |
|                 | <i>N1</i>  |                   |                   |                   |                   |
| 200 nm          | 39   | 481               | 1919              | >6000             | $>2 \times 10^4$  |
| 1 $\mu\text{m}$ | 4.4  | 54                | 211               | >700              | >2000             |
| 5 $\mu\text{m}$ | 0.8  | 9.4               | 37                | >150              | >400              |
|                 | <i>N3</i>  |                   |                   |                   |                   |
| 200 nm          | 0  | 10                | 100               | 270               | 614               |
| 1 $\mu\text{m}$ | 0  | 1.1               | 11                | 31                | 72                |
| 5 $\mu\text{m}$ | 0  | 0.2               | 1.9               | 5.5               | 13                |
|                 | <i>N10</i>   |                   |                   |                   |                   |
| 200 nm          | 0  | 0                 | 0                 | 3.4               | 246               |
| 1 $\mu\text{m}$ | 0  | 0                 | 0                 | 0.4               | 27                |
| 5 $\mu\text{m}$ | 0  | 0                 | 0                 | <0.1              | 4.8               |

<sup>a</sup>Dust concentrations are given in  $\text{cm}^{-3}$ .

was little higher for larger dust particles (mainly because the greater coagulational loss reduced the total condensation sink slightly as the simulation proceeded) the difference was around ten percent at most. The simplified size distribution representation for the dust particle mode therefore seems adequate for our theoretical study. It is also noteworthy that the sulphuric acid concentration quickly reached a concentration that led to soluble coating of mineral dust almost immediately after the beginning of the simulation. Choosing a bigger contact angle value (up to  $150^\circ$ ) delayed the formation of the coating only by some minutes.

[23] The criterion for inhibition of new particle formation was that at all times during the simulation the particle concentration in the nucleation mode remained below  $50 \text{ cm}^{-3}$ , corresponding to 5% of the particle concentration in Aitken and accumulation modes. The simulation results indicate that the sink required to prevent  $N_1$  formation increases rapidly with the sulphuric acid production rate and even at relatively low production rates exceeds  $0.01 \text{ s}^{-1}$ . The corresponding dust concentrations, shown in Table 1, are also unrealistically high. This suggests that apart from areas close to sources during strong dust events, mineral dust cannot typically prevent the formation of nanometer-sized clusters in the atmosphere. The result supports the hypothesis of *Kulmala et al.* [2000] according to which nucleation is ubiquitous in the troposphere but most of the time the thermodynamically stable clusters are unable to grow to detectable sizes.

[24] One should note that the critical measure of the dust loading in this study is condensational sink and not for example mass concentration, which typically is the quantity obtained from measurements. For example, the third column of data in Table 1 shows that either 1919 dust particles per  $\text{cm}^3$  of diameter 200 nm, or 37 dust particles per  $\text{cm}^3$  of diameter 5  $\mu\text{m}$  are needed to prevent particle formation altogether. Whereas the condensation sinks caused by these different sized particles are practically the same ( $1.03 \times 10^{-2} \text{ s}^{-1}$  for 200 nm particles,  $1.07 \times 10^{-2} \text{ s}^{-1}$  for 5  $\mu\text{m}$  particles), their mass concentrations differ by several orders of magnitude ( $16 \mu\text{g}/\text{m}^3$  for 200 nm

particles,  $4840 \mu\text{g}/\text{m}^3$  for 5  $\mu\text{m}$  particles). It is thus extremely difficult to compare our model results with measured total mass concentration values without any information on the actual particle sizes. Therefore we chose to report the model predicted dust loading as number concentration rather than as mass concentration, although the condensation sink caused by the dust particles could be calculated from either.

[25] To predict the dust load that prevents the growth of newly formed particles to 3 or 10 nm, we followed the particle size evolution for six hours after a short nucleation burst. Mimicking the burst, we initialized the nucleation mode with  $10^5 \text{ cm}^{-3}$  sulphuric acid-water particles of diameter 1.3 nm. This corresponds to the results of the homogeneous ternary nucleation model at simulation conditions. In the presence of pre-existing aerosol, particles of such small size are subject to strong coagulational loss. Detection of nucleated particles, however, necessitates that a sufficient concentration of them survive the growth to the detectable size. For the simulations, we chose a detection threshold concentration of  $10^2 \text{ cm}^{-3}$ . Therefore, even if newly formed particles managed to grow to sizes over 3 nm but at the same time their concentration was below the threshold value, we assumed that they could not be detected. In the base case simulations for growth to 10 nm, the nucleation mode concentration did not fall below the threshold value. This was a result of the substantially higher average growth rate and the fact that the coagulational loss slows down as the particles grow.

[26] Overall, the model predictions for critical initial sinks needed to inhibit the growth to 3 and 10 nm are highly more likely to be observed at atmospheric conditions than those for preventing nucleation (Figure 2). The same applies to the corresponding dust concentrations presented in Table 1, especially if one keeps in mind that only one size represents the whole dust distribution in the model. At high sulphuric acid production rates, condensation grows the pre-existing particles notably accelerating the coagulational loss of nucleated particles. Therefore, given the detection threshold concentration for the nucleation mode particles, the sink needed to prevent  $N_3$  formation approaches that needed to prevent  $N_{10}$  formation.

[27] Earlier studies have addressed the influence of nucleating vapor concentrations, pre-existing particle distribution and properties of the organic vapor on particle formation and growth [*Kerminen et al.*, 2001; *Pirjola et al.*, 2002]. *Kerminen et al.* [2001] also discuss the sensitivity of homogeneous nucleation to organic vapor production rates. Therefore we focus here on our simulation results concerning particle growth to detectable sizes, and test their sensitivity to the organic vapor production rate and the number concentration of nanometer-sized particles formed in the nucleation burst. For the sensitivity analysis, we chose a noontime maximum sulphuric acid production rate of  $1.4 \times 10^3 \text{ cm}^{-3} \text{ s}^{-1}$ .

[28] Because of the Kelvin effect, the organic vapor in the simulations could not condense on the particles immediately after they had formed. Therefore sulphuric acid was the only vapor condensing on the newly nucleated particles until they had grown to  $\sim 1.5\text{--}2.6$  nm in

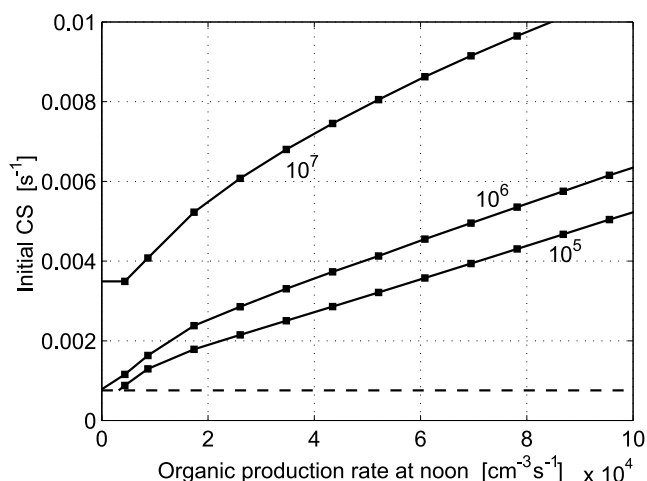


**Figure 3.** Critical initial condensation sinks that prevent the growth of nucleated particles to 3 nm as a function of their initial concentration ( $\text{cm}^{-3}$ ) and organic vapor production rate. The results are shown for substrate particles of 1  $\mu\text{m}$  in diameter. See text for detailed simulation conditions.

diameter, depending on the organic vapor concentration. Figure 3 illustrates that the critical sink that prevents particle detection at 3 nm is substantially higher for high organic production rates, the relationship between the two being almost linear at production rates above  $2 \times 10^4 \text{ cm}^{-3} \text{ s}^{-1}$ . Table 2 presents the dust concentrations corresponding to the lowest curve, i.e., to the case when initial particle concentration in the nucleation mode was  $10^5 \text{ cm}^{-3}$ . However, the initial concentration of nucleated particles strongly affects another mechanism determining the growth rate of nucleation mode particles, namely self-coagulation. The figure reveals that self-coagulation becomes important once the concentration of the nucleated particles exceeds  $10^6 \text{ cm}^{-3}$ . At concentrations as high as  $10^7 \text{ cm}^{-3}$ , this mechanism contributes to the growth of the newly formed particles effectively and can dominate over condensation. In order not to detect new particles at 3 nm, their coagulation loss onto pre-existing aerosol has to be very efficient. Therefore, when the topmost curve is compared to the lower two, the approximately twofold critical sinks result from the need for a higher coagulation

**Table 2.** Dust Concentrations Corresponding to Critical Initial Condensation Sinks in Figures 3 and 4 for Dust Particles of Diameter 200 nm, 1  $\mu\text{m}$ , and 5  $\mu\text{m}$ <sup>a</sup>

|                 | Maximum Organic Production Rate, $\text{cm}^{-3} \text{ s}^{-1}$ |                   |                   |                   |                   |
|-----------------|--|-------------------|-------------------|-------------------|-------------------|
|                 | $4.3 \times 10^3$  | $8.7 \times 10^3$ | $1.7 \times 10^4$ | $3.5 \times 10^4$ | $6.9 \times 10^4$ |
|                 | <i>N3</i>  |                   |                   |                   |                   |
| 200 nm          | 23   | 100               | 181               | 312               | 577               |
| 1 $\mu\text{m}$ | 2.5  | 10.8              | 21                | 35                | 64                |
| 5 $\mu\text{m}$ | 0.4  | 1.9               | 3.6               | 6.1               | 11                |
|                 | <i>N10</i>   |                   |                   |                   |                   |
| 200 nm          | 0  | 0                 | 42                | 223               | 535               |
| 1 $\mu\text{m}$ | 0  | 0                 | 4.6               | 24                | 60                |
| 5 $\mu\text{m}$ | 0  | 0                 | 0.8               | 4.2               | 11                |

<sup>a</sup>Dust concentrations are given in  $\text{cm}^{-3}$ .

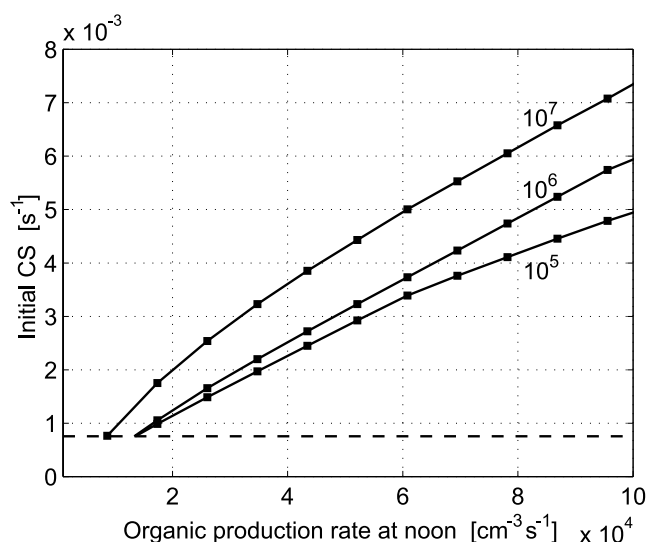


**Figure 4.** Critical initial condensation sinks that prevent the growth of nucleated particles to 10 nm as a function of their initial concentration ( $\text{cm}^{-3}$ ) and organic vapor production rate. The results are shown for substrate particles of 1  $\mu\text{m}$  in diameter. See text for detailed simulation conditions.

sink rather than a higher condensation sink. These two are, however, proportional to one another [Kulmala *et al.*, 2001a].

[29] The influence of self-coagulation on particle growth to 10 nm is less pronounced, yet prominent (Figure 4). The initial concentration of particles formed during the nucleation burst is of particular importance if the organic production rate is high. Then the fast condensational growth of pre-existing particles accelerates the coagulation loss of small particles. Therefore, if the initial concentration in the nucleation mode is low, it declines easily below the detection threshold concentration before the particles reach 10 nm in diameter. This explains why the lowest curve for critical condensation sinks bends at high organic production rate values. Again, Table 2 presents the dust concentrations corresponding to the case when the initial particle concentration in the nucleation mode was  $10^5 \text{ cm}^{-3}$ . One should note that although the dust concentrations in the table are relatively high, they are still within observable range especially close to dust source areas.

## 5. Conclusions

[30] In this study, we investigated ternary heterogeneous nucleation of water, sulphuric acid, and ammonia as a possible pathway leading to sulphate coating of mineral aerosol particles. The model simulations indicate that the nucleation energy barrier associated with the formation of sulphate embryos on dust particles is not the limiting factor of soluble coating. Therefore heterogeneous nucleation on dust can occur at atmospherically relevant conditions.

[31] We also addressed the effect of sulphate-coated mineral dust on the formation and growth of new aerosol particles. As the new particle formation route, we used



ternary homogeneous nucleation of water, sulphuric acid and ammonia vapors. In addition to sulphuric acid, condensation of organic vapors contributed to the growth of formed particles. A population of relatively large dust particles can, in principle, inhibit new particle formation in the atmosphere by acting as a condensation sink for nucleating vapors. According to our simulation results this seems not, however, to be the case, and new aerosol particles can form even in environments with high pre-existing dust concentrations. On the other hand, during dust events the growth of newly formed particles to detectable sizes (3 or 10 nm) can be strongly reduced in areas downwind of the dust source. Especially in desert regions, where organic vapor concentration is low, dust particles can easily suppress the formation of observable new particles. This is caused by dust particles acting as condensation sink for vapor molecules, thus hindering growth, or as coagulation sink for ultrafine aerosol particles, thus scavenging them out. This decoupling between nucleation and growth agrees with recent findings of *Kulmala et al.* [2000].

## References

- Adamson, A. W., *Physical Chemistry of Surfaces*, 4th ed., John Wiley, Hoboken, N. J., 1982.
- Alam, A., J. P. Shi, and R. M. Harrison, Observations of new particle formation in urban air, *J. Geophys. Res.*, 108(D3), 4093, doi:10.1029/2001JD001417, 2003.
- Andreae, M. O., Raising dust in the greenhouse, *Nature*, 380, 389–390, 1996.
- Arstila, H., P. Korhonen, and M. Kulmala, Ternary nucleation: Kinetics and application to water-ammonia-hydrochloric acid system, *J. Aerosol Sci.*, 30, 131–138, 1999.
- Ball, S. M., D. R. Hanson, and F. L. Eisele, Laboratory studies of particle nucleation: Initial results for H<sub>2</sub>SO<sub>4</sub>, H<sub>2</sub>O, and NH<sub>4</sub> vapor, *J. Geophys. Res.*, 104, 23,709–23,718, 1999.
- Chadwick, L. A., O. A. Derry, P. M. Vitousek, B. Huebert, and L. O. Hedin, Changing sources of nutrients during four million years of ecosystem development, *Nature*, 397, 491–497, 1999.
- Claquin, T., M. Schulz, Y. Balkanski, and O. Boucher, Uncertainties in assessing the radiative forcing by mineral dust, *Tellus, Ser. B*, 50, 491–505, 1998.
- Coale, K. H., et al., A massive phytoplankton bloom induced by an ecosystem-scale iron fertilization experiment in the equatorial Pacific Ocean, *Nature*, 383, 495–501, 1996.
- Coffman, D. J., and D. A. Hegg, A preliminary study of the effect of ammonia on particle nucleation in the marine boundary layer, *J. Geophys. Res.*, 100, 7147–7160, 1995.
- D'Almeida, G. A., and L. Schütz, Number, mass and volume distributions of mineral aerosol and soils of the Sahara, *J. Clim. Appl. Meteorol.*, 22, 233–243, 1983.
- Dentener, F. J., G. R. Carmichael, Y. Zhang, J. Lelieveld, and P. Crutzen, The role of mineral aerosol as a reactive surface in the global troposphere, *J. Geophys. Res.*, 101, 22,869–22,889, 1996.
- Duce, R. A., Sources, distributions, and fluxes of mineral aerosols and their relationship to climate, in *Aerosol Forcing of Climate*, edited by R. Charlson and J. Heintzenberg, pp. 43–72, John Wiley, Hoboken, N. J., 1995.
- Eisele, F., and D. Tanner, Measurement of the gas phase concentration of H<sub>2</sub>SO<sub>4</sub> and methane sulfonic acid and estimates of H<sub>2</sub>SO<sub>4</sub> production and loss in the atmosphere, *J. Geophys. Res.*, 98, 9001–9010, 1993.
- Fletcher, N. H., Size effect in heterogeneous nucleation, *J. Chem. Phys.*, 29, 572–576, 1958.
- Fuchs, N. A., *The Mechanics of Aerosols*, Pergamon, New York, 1964.
- Fuchs, N. A., and A. G. Sutugin, Highly dispersed aerosol, in *Topics in Current Aerosol Research*, edited by G. M. Hidy and J. R. Brock, pp. 1–60, Pergamon, New York, 1971.
- Gomes, L., G. Bergametti, G. Coude-Gaussan, and P. Rognon, Submicron desert dusts: A sandblasting process, *J. Geophys. Res.*, 95, 13,927–13,935, 1990.
- Hamill, P., R. P. Turco, C. S. Kiang, O. B. Toon, and R. C. Whitten, An analysis of various nucleation mechanisms for sulfate particles in the stratosphere, *J. Aerosol Sci.*, 6, 561–585, 1982.
- Intergovernmental Panel on Climate Change (IPCC), *Climate Change 2001: The Scientific Basis. Contribution of Working Group I to the Third Assessment Report of the Intergovernmental Panel on Climate Change*, edited by J. T. Houghton et al., 881 pp., Cambridge Univ. Press, New York, 2001.
- Kerminen, V.-M., A. Virkkula, R. Hillamo, A. S. Wexler, and M. Kulmala, Secondary organics and atmospheric cloud condensation nuclei production, *J. Geophys. Res.*, 105, 9255–9264, 2000.
- Kerminen, V.-M., L. Pirjola, and M. Kulmala, How significantly does coagulation scavenging limit atmospheric particle production?, *J. Geophys. Res.*, 106, 24,119–24,125, 2001.
- Kulmala, M., L. Pirjola, and J. M. Mäkelä, Stable sulphate clusters as a source of new atmospheric particles, *Nature*, 404, 66–69, 2000.
- Kulmala, M., M. Dal Maso, J. M. Mäkelä, L. Pirjola, M. Väkevä, P. Aalto, P. Mikkulainen, K. Hämeri, and C. O'Dowd, On the formation, growth and composition of nucleation mode particles, *Tellus, Ser. B*, 53, 479–490, 2001a.
- Kulmala, M., et al., Overview of the International Project on Biogenic Aerosol Formation in the Boreal Forest (BIOFOR), *Tellus, Ser. B*, 53, 324–343, 2001b.
- Kulmala, M., A. Lauri, H. Vehkamäki, A. Laaksonen, D. Petersen, and P. E. Wagner, Strange predictions by binary heterogeneous nucleation theory compared with quantitative experiment, *J. Phys. Chem. B*, 105, 11,800–11,808, 2001c.
- Laaksonen, A., and D. W. Oxtoby, Gas-liquid nucleation of nonideal binary mixtures: I. A density functional study, *J. Chem. Phys.*, 102, 5803–5810, 1995.
- Lazaridis, M., M. Kulmala, and A. Laaksonen, Binary heterogeneous nucleation of a water-sulphuric acid system: The effect of hydrate interaction, *J. Aerosol Sci.*, 7, 823–830, 1991.
- Levin, Z., E. Gaynor, and V. Gladstein, The effects of desert particles coated with sulfate on rain formation in the Eastern Mediterranean, *J. Appl. Meteorol.*, 35, 1511–1523, 1996.
- Liao, H., and J. H. Seinfeld, Radiative forcing by mineral dust aerosols: Sensitivity to key variables, *J. Geophys. Res.*, 103, 31,637–31,646, 1998.
- Martin, J. A., Iron still comes from above, *Nature*, 353, 123, 1991.
- Napari, I., M. Noppel, H. Vehkamäki, and M. Kulmala, An improved model for ternary nucleation of sulfuric acid-ammonia-water, *J. Chem. Phys.*, 116, 4221–4227, 2002.
- O'Dowd, C., et al., A dedicated study of New Particle Formation and Fate in the Coastal Environment (PARFORCE): Overview of objectives and achievements, *J. Geophys. Res.*, 107(D19), 8108, doi:10.1029/2001JD00055, 2002.
- Pirjola, L., and M. Kulmala, Aerosol dynamical model MULTIMONO, *Boreal Environ. Res.*, 5, 361–374, 2000.
- Pirjola, L., and M. Kulmala, Development of particle size and composition distribution with a novel aerosol dynamics model, *Tellus, Ser. B*, 53, 491–509, 2001.
- Pirjola, L., H. Korhonen, and M. Kulmala, Condensation/evaporation of insoluble organic vapor as functions of source rate and saturation vapor pressure, *J. Geophys. Res.*, 107(D11), 4108, doi:10.1029/2001JD001228, 2002.
- Pirjola, L., S. Tsyro, L. Tarrason, and M. Kulmala, A monodisperse aerosol dynamics module, a promising candidate for use in long-range transport models: Box model tests, *J. Geophys. Res.*, 108(D9), 4258, doi:10.1029/2002JD002867, 2003.
- Prospero, J. M., M. Uematsu, and D. L. Savoie, Mineral aerosol transport to the Pacific Ocean, in *Chemical Oceanography*, vol. 10, edited by J. P. Riley, R. Chester, and R. A. Duce, pp. 188–218, Academic, San Diego, Calif., 1989.
- Schack, C. J., Jr., S. E. Pratsinis, and S. K. Friedlander, A general correlation for deposition of suspended particles from turbulent gases to completely rough surfaces, *Atmos. Environ.*, 19, 953–960, 1985.
- Schütz, L., R. Jaenicke, and H. Pietrik, Saharan dust transport over the North Atlantic Ocean, *Spec. Pap. Geol. Soc. Am.*, 186(18), 87–100, 1981.
- Seinfeld, J. H., and S. N. Pandis, *Atmospheric Chemistry and Physics: From Air Pollution to Climate Change*, John Wiley, Hoboken, N. J., 1998.
- Sokolik, I., and O. B. Toon, Dust radiative forcing by anthropogenic airborne mineral aerosols, *Nature*, 381, 681–683, 1996.
- Sokolik, I. N., D. M. Winker, G. Bergametti, D. A. Gillette, G. Carmichael, Y. I. Kaufman, L. Gomes, L. Schuetz, and J. E. Penner, Introduction to special section: Outstanding problems in quantifying the radiative impacts of mineral dust, *J. Geophys. Res.*, 106, 18,015–18,027, 2001.
- Tang, I. N., and H. R. Munkelwitz, Water activities, densities, and refractive indices of aqueous sulfates and sodium nitrate droplets of atmospheric importance, aerosol, *J. Geophys. Res.*, 99, 18,801–18,808, 1994.
- Tegen, I., and I. Fung, Contribution to the mineral aerosol load from land surface modification, *J. Geophys. Res.*, 100, 18,707–18,726, 1995.
- Tegen, I., and A. A. Lacis, Modeling of particle size distribution and its influence on the radiative properties of mineral dust aerosol, *J. Geophys. Res.*, 101, 19,237–19,244, 1996.



- Tegen, I., A. A. Lacis, and I. Fung, The influence on climate forcing of mineral aerosols from disturbed soils, *Nature*, 380, 419–422, 1996.
- Underwood, G. M., C. H. Song, M. Phadnis, G. R. Carmichael, and V. H. Grassian, Heterogeneous reactions of NO<sub>2</sub> and HNO<sub>3</sub> on oxides and mineral dust: A combined laboratory and modeling study, *J. Geophys. Res.*, 106, 18,055–18,066, 2001.
- Weber, R. J., J. J. Marti, P. H. McMurry, F. L. Eisele, D. J. Tanner, and A. Jefferson, Measurements of new particle formation and ultrafine particle growth rates at a clean continental site, *J. Geophys. Res.*, 102, 4375–4385, 1997.
- Wurzler, S., T. G. Reisin, and Z. Levin, Modification of mineral dust particles by cloud processing and subsequent effects on drop size distributions, *J. Geophys. Res.*, 105, 501–512, 2000.
- Zhang, Y., and G. R. Carmichael, The role of mineral aerosol in tropospheric chemistry in East-Asia: A model study, *J. Appl. Meteorol.*, 101, 22,869–22,889, 1999.

---

H. Korhonen, M. Kulmala, A. Lauri, K. E. J. Lehtinen, I. Napari, L. Pirjola, and H. Vehkamäki, Department of Physical Sciences, University of Helsinki, P. O. Box 64, FIN-00014 University of Helsinki, Finland. (hannele.s.korhonen@helsinki.fi; kulmala@pcu.helsinki.fi; antti.lauri@helsinki.fi; kari.lehtinen@helsinki.fi; ismo.napari@helsinki.fi; liisa.pirjola@helsinki.fi; hanna.vehkamaki@helsinki.fi)

C. Timmreck, Max-Planck-Institut für Meteorologie, Bundesstraße 55, D-20146 Hamburg, Germany. (timmreck@dkrz.de)